PERGAMON

Computers and Structures 80 (2002) 1881–1894

Computers & Structures

www.elsevier.com/locate/compstruc

Identification of damage locations for plate-like structures using damage sensitive indices: strain modal approach

Y.Y. Li [a,b,*], L. Cheng [a], L.H. Yam [a], W.O. Wong [a]

[a] Department of Mechanical Engineering, The Hong Kong Polytechnic University, Hung Hom, Kowloon, Hong Kong SAR, China
[b] Department of Mechanical Engineering, Fuzhou University, 350002, PR China

Received 19 October 2001; accepted 8 July 2002

Abstract

This paper addresses the problem of identification of damage locations for plate-like structures using strain mode technique. Based on the Rayleigh–Ritz approach, the strain modal analysis of a damaged plate is performed and strain mode shapes are consequently obtained. In light of the continuity condition and the residual strain mode shape technique, two novel damage sensitive parameters are proposed to determine the locations of damage, and corresponding damage indices are constructed. Compared with the conventional indices, they are simple and intuitive, and easy to be used in practice. Numerical simulations and experiments are carried out. Results show a good consistency and a strong identification capability of the proposed indices.

Keywords: Strain mode shape; Damage sensitive index; Plate-like structure; Rayleigh–Ritz method

1. Introduction

An important topic in mechanical, aeronautic and structural engineering application is the detection of damage occurring in structures, which affects structural safety, reliability and operational life [1–3]. Usually, damage detection includes the determination of the existence of damage, the location identification and the severity estimation. Among these three stages, the identification of damage locations is the foundation of damage repair and control, which has received considerable attention and leads to a rapid development of many techniques in recent years [4–7].

Damage index approach by constructing indices from various modal parameters, as one of the most effective methods for damage location identification, has been extensively adopted [8–11]. Ahmadian et al. formulated two damage location indicators from the condition number using substructure mode shapes [8]. Cornwell et al. defined the damage index using the strain energy approach, in which the information of mode shapes of the structure before and after damage are required [9]. Dems and Mroz proposed that the frequency variation can be adopted in assessing the location and magnitude of damage by introducing the damage indices [10]. These indices have shown to be very reliable for location assessment. The existing problem is that the establishment of some indices, for example, indices from the condition number, requires a complicated computation, and is difficult to be realized in many practical applications. Moreover, some indices, such as the index from the change in natural frequency, are insensitive to incipient damage in the structure. In view of this, some simple and

* Corresponding author. Address: Department of Mechanical Engineering, The Hong Kong Polytechnic University, Hung Hom, Kowloon, Hong Kong SAR, China. Tel.: +852-2766-6681; fax: +852-2365-4703.
E-mail address: mmyylee@polyu.edu.hk (Y.Y. Li).

0045-7949/02/$ - see front matter
PII: S0045-7949(02)00209-2

effective indices need to be developed with the help of proper selection of damage sensitive parameters.

As is known, strain (or curvature) mode shape is a sensitive parameter to damage because of its local behaviour [12,13], and has been utilized to locate damage sites in beams or frame structures [14–17]. When it is used to identify damage in complex structural systems, such as the plate-like structures, some issues will be of great interest, e.g., the establishment of an intuitive and effective damage sensitive index, the achievement of an accurate strain mode shape, and etc. Cornwell et al. detected damage locations in plate-like structures based on the changes in strain energy, which is related to the change in the curvature of mode shapes [9]. Swamidas and Chen discovered qualitatively that the difference of the strain mode shape is a sensitive parameter to damage [18]. However, there is no existing report on systematical and quantitative analysis concerning the selection of damage sensitive parameters, the construction of damage index and the description of the strain mode shape.

The aim of this paper is to investigate these problems in detail. The outline of this paper is as follows. In Section 2, the strain modal analysis of the damaged plate is performed, and the strain mode shape used for the construction of damage index is derived using the Rayleigh–Ritz approach. In Section 3, with the help of the continuity condition and the residual strain mode shape technique, two novel indices—the bending moment index $\bar{\beta}_{r,x}(x,y)$ and the residual strain mode shape index $\Delta\bar{\varepsilon}_{r,x}(x,y)$, are proposed to locate damage sites in plate-like structures. In Section 4, numerical simulations of a simply supported plate with different number and locations of damage are performed. Experimental verifications are carried out in Section 5, showing a good agreement with the theoretical analysis. Finally, conclusions are drawn.

2. Strain modal analysis of damaged plates

Since the achievement of an accurate strain mode shape is the foundation for the construction of damage indices using strain mode technique, the strain modal analysis of a damaged plate is carried out in this section. To analytically investigate the change in strain mode shapes at the damage site, vibration analysis of a damaged plate is first investigated. Usually, different kinds of damage, such as crack and corrosion cause a local stiffness reduction so as to affect the structural behaviour. In this paper, this type of damage is simulated by a defective area of the plate with a reduced thickness.

2.1. Vibration analysis of damaged plates

Consider the free vibration of a rectangular plate $(a \times b \times h)$ with damage locating at the defective area $\boldsymbol{S}_{\mathrm{d}}$ ($\boldsymbol{S}_{\mathrm{d}} = [x_1 x_2] \times [y_1 y_2]$) (Fig. 1(a)). In view of the continuity conditions of the bending moment $M_x(x,y)$ and the transverse shearing force $V_x(x,y)$ at the interface between the non-defective and defective regions, we have

$$M_x^+(x,y)\big|_{\substack{x=x_1^+\\ x=x_2^+}} = M_x^-(x,y)\big|_{\substack{x=x_1^-\\ x=x_2^-}}, \tag{1a}$$

$$V_x^+(x,y)\big|_{\substack{x=x_1^+\\ x=x_2^+}} = V_x^-(x,y)\big|_{\substack{x=x_1^-\\ x=x_2^-}}, \tag{1b}$$

where

$$M_x(x,y) = -D(x,y)\left(\frac{\partial^2 W(x,y)}{\partial x^2} + v\frac{\partial^2 W(x,y)}{\partial y^2}\right), \tag{2a}$$

$$V_x(x,y) = -D(x,y)\frac{\partial}{\partial x}\left(\frac{\partial^2 W(x,y)}{\partial x^2} + \frac{\partial^2 W(x,y)}{\partial y^2}\right), \tag{2b}$$

where $D(x,y)$ is the variable flexural rigidity, which can be obtained by defining the general location function $\chi_\gamma(x,y)$ as

$$\chi_\gamma(x,y) = \begin{cases} 1, & (x,y) \notin \boldsymbol{S}_{\mathrm{d}}, \\ 1 - \frac{h_{\mathrm{c}}}{h}, & (x,y) \subset \boldsymbol{S}_{\mathrm{d}}, \end{cases} \tag{3}$$

i.e.,

$$D(x,y) = D_0\chi_r^3(x,y), \quad D_0 = \frac{Eh^3}{12(1-v^2)}, \tag{4}$$

where E and v are the elastic modulus and the Poisson ratio, respectively, h_{c} is the depth of damage and $0 < h_{\mathrm{c}}/h < 1$. In Eqs. (2a) and (2b), $W(x,y)$ is the mode shape function expressed by a series as [19]

$$W(x,y) = \sum_{i=1}^{m}\sum_{j=1}^{n} c_{ij}\varphi_i(x)\eta_j(y), \tag{5}$$

where $\varphi_i(x)$ and $\eta_j(y)$ are appropriate admissible functions, c_{ij} are the unknown coefficients. In light of the strain–displacement relationship, one can define the "strain mode shape" as the distribution of the in-plane strain components at the top or bottom surface of the plate according to the corresponding natural vibration mode. For example, the strain mode shape in the x and y directions can be expressed as

$$\varepsilon_x(x,y) = -h\chi_r(x,y)\frac{\partial^2 W(x,y)}{\partial x^2}, \tag{6a}$$

$$\varepsilon_y(x,y) = -h\chi_r(x,y)\frac{\partial^2 W(x,y)}{\partial y^2}. \tag{6b}$$

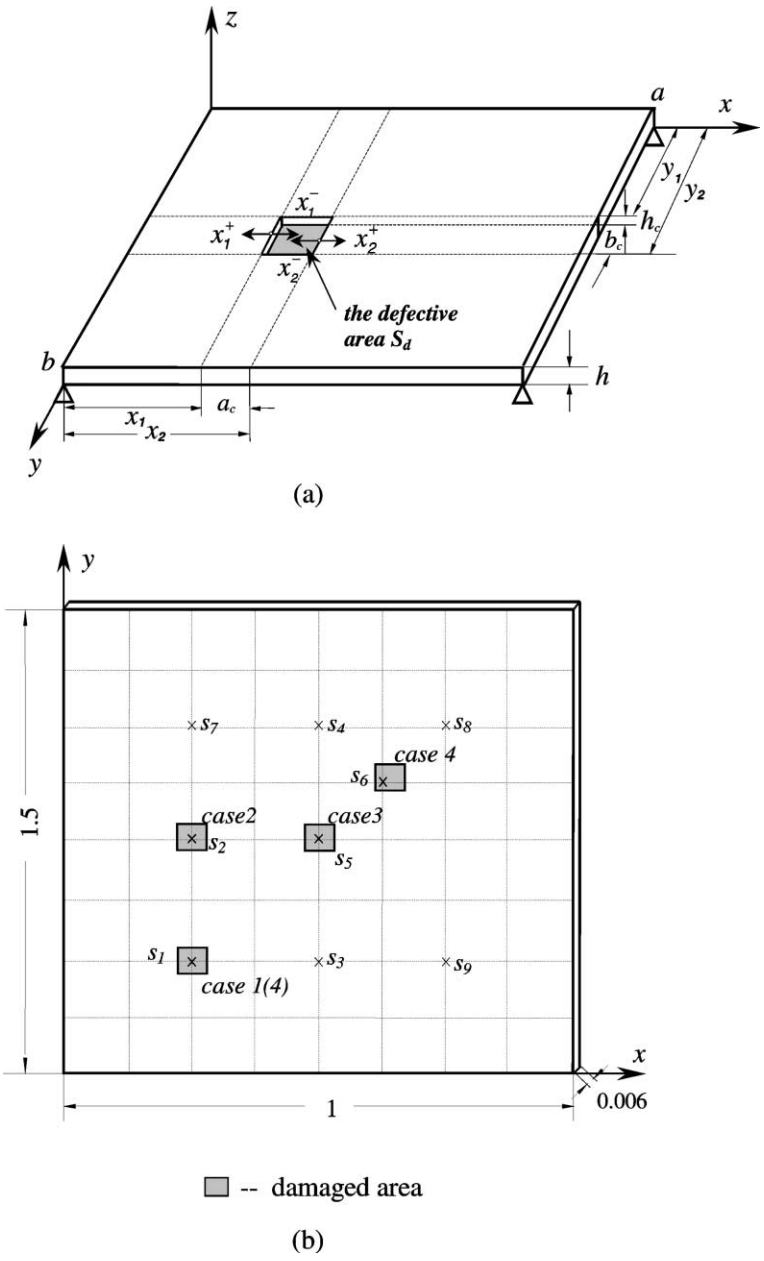

Fig. 1. (a) The schematic diagram of a simply supported plate with damage occurring at $\boldsymbol{S}_{\mathrm{d}}$. (b) Four cases of damage locations.

Combining Eqs. (1a)–(2b) and (6a) results in the following equation,

$$\varepsilon_x^+(x,y)\big|_{\substack{x=x_1^+\\x=x_2^+}} = (1-h_c/h)\varepsilon_x^-(x,y)\big|_{\substack{x=x_1^-\\x=x_2^-}}. \tag{7}$$

It is clear that (discussion is focused on $\varepsilon_x(x,y)$, similar results can be obtained for $\varepsilon_y(x,y)$):

- For the intact case ($h_c/h=0$), $D(x,y)$ is a constant and $\varepsilon_x^+(x,y)=\varepsilon_x^-(x,y)$. It implies that the curve surface of $\varepsilon_x(x,y)$ is continuous and smooth.
- For the damaged case ($0<h_c/h<1$), the sudden change of h at the defective area leads to the appearance of significant variations in $\varepsilon_x(x,y)$, and with the increase of h_c, i.e., the exacerbation of damage, this phenomenon tends to be significant.

- Change in strain mode shape will be trivial outside the defective area.

Apparently, this local characteristic of the strain mode shape can be adopted to identify damage locations in plate-like structures.

2.2. Derivation of strain mode shapes for the damaged plate

According to Eqs. (6a) and (6b), the strain mode shape can be obtained by taking partial derivative on the corresponding $W(x,y)$ with respect to Cartesian coordinates. Based on this fact, the determination of the unknown coefficients c_{ij} in Eq. (5) is the essential step for the achievement of an accurate strain mode shape. By using the Rayleigh–Ritz method, c_{ij} can be obtained by solving the minima of the energy function $J(W)$ as

$$\begin{aligned}\frac{\partial J(W)}{\partial c_{ij}} &= \frac{\partial}{\partial c_{ij}}\left\{\int_0^a\int_0^b \frac{D(x,y)}{2}\left[\left(\frac{\partial^2 W(x,y)}{\partial x^2}+\frac{\partial^2 W(x,y)}{\partial y^2}\right)^2\right.\right.\\ &\quad -2(1-v)\left(\frac{\partial^2 W(x,y)}{\partial x^2}\frac{\partial^2 W(x,y)}{\partial y^2}\right.\\ &\quad \left.\left.\left.-\left(\frac{\partial^2 W(x,y)}{\partial x\,\partial y}\right)^2\right)\right]\mathrm{d}y\,\mathrm{d}x\\ &\quad \left.-\frac{\omega^2}{2}\int_0^a\int_0^b \gamma\chi_\gamma(x,y)W^2(x,y)\,\mathrm{d}y\,\mathrm{d}x\right\}=0,\end{aligned} \tag{8}$$

where ω and γ are the modal frequency of the plate and the mass of the plate per unit area, respectively. Eq. (8) implies that the occurrence of damage in a plate-like structure is regarded as the loss of energy, and the influence of damage on mode shape herein will be embodied by c_{ij} through the variable $D(x,y)$. Substituting Eq. (5) into (8) and denoting that

$$E_{ik}^{(r,s)}=\begin{cases}\int_0^{x_1}\frac{\mathrm{d}^r\varphi_i(x)}{\mathrm{d}x^r}\frac{\mathrm{d}^s\varphi_k(x)}{\mathrm{d}x^s}\,\mathrm{d}x, & 0\leqslant x<x_1,\\ \frac{(h-h_c)^3}{h^3}\int_{x_1}^{x_2}\frac{1}{\chi_\gamma^3(x,y)}\frac{\mathrm{d}^r\varphi_i(x)}{\mathrm{d}x^r}\frac{\mathrm{d}^s\varphi_k(x)}{\mathrm{d}x^s}\,\mathrm{d}x, & x_1\leqslant x\leqslant x_2,\\ \int_{x_2}^{a}\frac{\mathrm{d}^r\varphi_i(x)}{\mathrm{d}x^r}\frac{\mathrm{d}^s\varphi_k(x)}{\mathrm{d}x^s}\,\mathrm{d}x, & x_2<x\leqslant a,\end{cases}\quad i,k=1,\ldots,m, \tag{9}$$

$$F_{jl}^{(r,s)}=\int_0^b\frac{\mathrm{d}^r\eta_j(y)}{\mathrm{d}y^r}\frac{\mathrm{d}^s\eta_l(y)}{\mathrm{d}y^s}\,\mathrm{d}y,\quad j,l=1,\ldots,n, \tag{10}$$

$$G_{ik}^{(0,0)}=\begin{cases}\int_0^{x_1}\varphi_i(x)\varphi_k(x)\,\mathrm{d}x, & 0\leqslant x<x_1,\\ \left(1-\frac{h_c}{h}\right)\int_{x_1}^{x_2}\frac{1}{\chi_\gamma(x,y)}\varphi_i(x)\varphi_k(x)\,\mathrm{d}x, & x_1\leqslant x\leqslant x_2,\\ \int_{x_2}^{a}\varphi_i(x)\varphi_k(x)\,\mathrm{d}x, & x_2<x\leqslant a,\end{cases} \tag{11}$$

$$m_{ij,kl}=G_{ik}^{(0,0)}F_{jl}^{(0,0)}, \tag{12}$$

$$\begin{aligned}k_{ij,kl}&=E_{ik}^{(2,2)}F_{jl}^{(0,0)}+E_{ik}^{(0,0)}F_{jl}^{(2,2)}+v(E_{ik}^{(2,0)}F_{jl}^{(0,2)}+E_{ik}^{(0,2)}F_{jl}^{(2,0)})\\ &\quad+2(1-v)E_{ik}^{(1,1)}F_{jl}^{(1,1)},\end{aligned} \tag{13}$$

we have the following matrix expression,

$$\begin{bmatrix}k_{11,11}-\lambda^2 m_{11,11} & \cdots & k_{mn,11}-\lambda^2 m_{mn,11}\\ \cdots & \cdots & \cdots\\ k_{11,mn}-\lambda^2 m_{11,mn} & \cdots & k_{mn,mn}-\lambda^2 m_{mn,mn}\end{bmatrix}\begin{Bmatrix}c_{11}\\ \vdots\\ c_{mn}\end{Bmatrix}=\mathbf{0}, \tag{14}$$

where $\lambda^2=(\gamma/D_0)^{1/2}\omega a^2$ is the frequency parameter. It is known that the characteristic equation resulting from Eq. (14) has $m\times n$ roots, corresponding to $m\times n$ natural frequencies and $m\times n$ mode shapes. Using one of these $m\times n$ roots, called mode r, the corresponding $c_{r,ij}$ coefficients are determined. Thereby, the rth strain mode shape of the damaged plate can be derived. It should also be pointed out that only relative values of $c_{r,ij}$ can be determined. Thus, all quantities derived from them ought to be appropriately scaled.

According to the Rayleigh–Ritz method, the assumed strain function $\varepsilon_{r,x}(x,y)$ in Eqs. (6a) and (6b) (or displacement function $W(x,y)$ in Eq. (5)) approaches the exact solution as (m,n) approach infinity under the condition that the admissible functions $\varphi_i(x)$ and $\eta_j(y)$ satisfy [19,20]: (1) $\varphi_i(x)$ and $\eta_j(y)$ are linearly independent; (2) each of $\varphi_i(x)$ and $\eta_j(y)$ forms a complete system of functions, and (3) they satisfy the geometric boundary conditions in the x and y directions, respectively. Consider that the low-frequency modes can furnish adequate information for damage location identification, the number of terms should be selected properly so that a high accuracy of results can be guaranteed within the frequency range of interest. An effective way to select N (N stands for a combination of m and n) is described as follows:

Given a small threshold value δ, if the tolerance Δ (Δ is the maximal difference between $\varepsilon_{r,x}(x,y)$ with $N+1$ and N terms in the series expansion among the analyzed modes) converges to δ, then N will be chosen as the orders of the series in Eq. (5).

3. Sensitive indices for damage location identification

As has already been pointed out, the strain mode shape is a sensitive parameter for locating damage sites in plate-like structures. The construction of damage indicators using the measured information of strain mode shape is dealt with, and two novel damage sensitive indices are presented in the following sections.

3.1. Bending moment index

According to the continuity condition of the bending moment (Eqs. (1a) and (2a)), for the rth vibration mode, one has

$$\left(\varepsilon^{+}_{r,x}(x,y)+v\varepsilon^{+}_{r,y}(x,y)\right)\Big|_{\substack{x=x^{+}_{1}\\ x=x^{+}_{2}}} = (1-h_c/h)\left(\varepsilon^{-}_{r,x}(x,y)+v\varepsilon^{-}_{r,y}(x,y)\right)\Big|_{\substack{x=x^{-}_{1}\\ x=x^{-}_{2}}}. \tag{15}$$

Define the bending moment parameter as

$$\beta_{r,x}(x,y)=\varepsilon_{r,x}(x,y)+v\varepsilon_{r,y}(x,y), \tag{16}$$

it is evident that $\beta_{r,x}(x,y)$ is sensitive to damage, and is therefore adopted to construct the bending moment index as

$$\bar{\beta}_{r,x}(x,y)=\frac{\left|\beta_{r,x}(x,y)\right|}{\max\left|\beta_{r,x}(x,y)\right|}. \tag{17}$$

This is an intuitive way for locating damage sites without requiring the measured information of the strain mode shape of the intact case. An easy implementation of this method is to attach strain gauges to some critical areas of the structure to measure the relative amplitudes of strains, which are directly related to strain mode shapes.

When the bending moment index is used for damage location identification, the problem considered is that peaks appear not only at the defective area, but also at those positions where the extreme amplitudes of modes are found. In order to reduce the 'neglect alarm' to a low level, the following identification procedure is proposed:

Step 1. By using the vibration test, i.e., exciting the analyzed structure with the rth natural frequency, the relative amplitudes of strains at the measurement locations are recorded to form the bending moment index $\bar{\beta}_{r,x}(x,y)$.

Step 2. Searching the locations $(s_1,\ldots,s_i,\ldots,s_l)$ of significant variations of $\bar{\beta}_{r,x}(x,y)$, and determining the aggregation $(\boldsymbol{S}_p)_r$ of locations at peaks for the rth strain mode. Then, checking whether s_i is not the element of $(\boldsymbol{S}_p)_r$, i.e., whether the condition $s_i\cap(\boldsymbol{S}_p)_r=\emptyset$ is satisfied. If it is the case, no intersection between s_i and $(\boldsymbol{S}_p)_r$ will be found. According to the local behaviour of the parameter of bending moment, s_i must be the location of damage; otherwise, it may be the peak of the rth mode.

Step 3. Re-exciting the structure with another frequency to judge the nature of s_i, and repeating these procedures till all potential damage locations are analyzed.

Next, the selection of parameter $\beta_{r,x}(x,y)$ for the construction of the damage index is investigated. To analyze the sensitivity of parameters $\varepsilon_{r,x}(x,y)$ and $\beta_{r,x}(x,y)$ to damage sites, the degrees of changes in these parameters at the interface between the non-defective and defective areas are given by

$$\alpha_{\varepsilon_r}=1-\frac{\varepsilon^{+}_{r,x}(x=x^{+},y)}{\varepsilon^{-}_{r,x}(x=x^{-},y)}=h_c/h \tag{18}$$

and

$$\alpha_{\beta_r}=1-\frac{\beta^{+}_{r,x}(x=x^{+},y)}{\beta^{-}_{r,x}(x=x^{-},y)}=h_c/h. \tag{19}$$

A comparison between Eqs. (18) and (19) shows that both $\beta_{r,x}(x,y)$ and $\varepsilon_{r,x}(x,y)$ are sensitive parameters for damage location identification. However, $\beta_{r,x}(x,y)$ will give stronger indication of damage location than that given by $\varepsilon_{r,x}(x,y)$, because the signal of the former is the superposition of $\varepsilon_{r,x}(x,y)$ and $\varepsilon_{r,y}(x,y)$ (Eq. (16)), and is thus stronger than the latter. For this reason, the bending moment is more sensitive in detecting damage than the strain mode shape, and it is therefore appropriate to select $\beta_{r,x}(x,y)$ for the construction of the damage sensitive index.

3.2. Residual strain mode shape index

The concept of the residue strain mode shape is from the difference of the curvature of the same order mode shape between the intact and damaged cases. In general, it can be written in the form as

$$\begin{aligned}\Delta\varepsilon_{r,x}(x,y)&=\varepsilon_{r,x}(x,y)-(\varepsilon_u)_{r,x}(x,y)\\&=\sum_{i=1}^{m}\sum_{j=1}^{n}h\chi_\gamma(x,y)\left[(c_u)_{r,ij}-c_{r,ij}\right]\varphi_i''(x)\eta_j(y)\\&=[\psi(x,y)]\{C_r\},\end{aligned} \tag{20}$$

where $(\varepsilon_u)_{r,x}(x,y)$ and $(c_u)_{r,ij}$ are the correspondence of $\varepsilon_{r,x}(x,y)$ and $c_{r,ij}$ for the intact case, and

$$[\psi(x,y)]=\left[\varphi_1''(x)\eta_1(y),\ldots,\varphi_1''(x)\eta_n(y),\ldots,\varphi_m''(x)\eta_1(y),\ldots,\varphi_m''(x)\eta_n(y)\right]_{1\times mn}, \tag{21a}$$

$$\{C_r\}=h\chi_\gamma(x,y)\{c_{r,11}-(c_u)_{r,11},\ldots,c_{r,1n}-(c_u)_{r,1n}\ldots,c_{r,m1}-(c_u)_{r,m1},\ldots,c_{r,mn}-(c_u)_{r,mn}\}^{\mathrm{T}}. \tag{21b}$$

Similar to the construction of the bending moment index, the residual strain mode shape index can be defined as

$$\Delta\bar{\varepsilon}_{r,x}(x,y)=\frac{\left|\Delta\varepsilon_{r,x}(x,y)\right|}{\max\left|\Delta\varepsilon_{r,x}(x,y)\right|}. \tag{22}$$

Thus, damage locations in the plate-like structure will be found from peaks of $\Delta\bar{\varepsilon}_{r,x}(x,y)$. That is to say, they will appear at those locations satisfying

$$\frac{\partial \Delta\varepsilon_{r,x}(x,y)}{\partial x} = 0 \quad \text{and} \quad \frac{\partial \Delta\varepsilon_{r,x}(x,y)}{\partial y} = 0. \tag{23}$$

Since the construction of the index $\Delta\bar{\varepsilon}_{r,x}(x,y)$ is based on the subtraction approach, the influence of peaks caused by modes on the identification result will be eliminated. This is a simple way for damage location identification from vibration test. The only deficiency is that it requires the strain measurement of the intact structure.

The above analysis is for the identification of damage locations using the information of the rth mode. In order to reveal the relationship between the identification result and the selection of different modes, the following derivation is presented.

Assume that the elements of $[\psi(x,y)]$ in Eq. (20) are not equal to zero simultaneously, i.e., damage does not locate at the nodal line. Then, the general expression of $\{C_r\}$ can be given by

$$\{C_r\} = [\psi(x,y)]^{+}\Delta\varepsilon_{r,x}(x,y), \tag{24}$$

where $[\psi(x,y)]^{+} = [\psi(x,y)]^{\mathrm{T}}([\psi(x,y)][\psi(x,y)]^{\mathrm{T}})^{-1}$ is the pseudo-inverse of $[\psi(x,y)]$.

Substituting Eqs. (20) and (24) into (23) yields

$$\begin{cases} \dfrac{\partial[\psi(x,y)]}{\partial x}[\psi(x,y)]^{+}\Delta\varepsilon_{r,x}(x,y) = 0, \\ \dfrac{\partial[\psi(x,y)]}{\partial y}[\psi(x,y)]^{+}\Delta\varepsilon_{r,x}(x,y) = 0. \end{cases} \tag{25}$$

To investigate the number and location of peaks at the defective area for different modes, the equivalent equations of Eq. (25) for the i and jth modes are formed to construct the objective function as

$$\prod : \begin{cases} \dfrac{\partial[\psi(x,y)]}{\partial x}[\psi(x,y)]^{+}\left(\Delta\varepsilon_{i,x}(x,y) - \mu_j\Delta\varepsilon_{j,x}(x,y)\right) = 0, \\ \dfrac{\partial[\psi(x,y)]}{\partial y}[\psi(x,y)]^{+}\left(\Delta\varepsilon_{i,x}(x,y) - \mu_j\Delta\varepsilon_{j,x}(x,y)\right) = 0, \end{cases} \tag{26}$$

where μ_j is the weighting function. Since damage locates away from the nodal line, the conditions

$$\frac{\partial[\psi(x,y)]}{\partial x}[\psi(x,y)]^{+} \neq 0 \quad \text{and} \quad \frac{\partial[\psi(x,y)]}{\partial y}[\psi(x,y)]^{+} \neq 0$$

hold. In such case, the solution of Eq. (26) satisfies $\Delta\varepsilon_{i,x}(x,y) - \mu_j\Delta\varepsilon_{j,x}(x,y) = 0$. It shows implicitly that the number and location of peaks are the same for different modes. That is, they are independent of the selected modal order for analysis.

In particular, when all the elements of $[\psi(x,y)]$ become zero, $[\psi(x,y)]^{+}$ does not exist and it is untenable to analyze the number and location of peaks using Eq. (26). This case happens when damage locates at the nodal line of the mode. Under this circumstance, for mode r, peaks appear at those locations that make

$$\frac{\partial[\psi(x,y)]}{\partial x}\{C_r\}\bigg|_{y\neq y_r} = 0 \quad \text{and} \quad \frac{\partial[\psi(x,y)]}{\partial y}\{C_r\}\bigg|_{x\neq x_r} = 0 \tag{27}$$

hold simultaneously, x_r, y_r being the nodal lines of mode r if they exist. Obviously, the number and location of peaks are variable for different modes.

One problem to be mentioned is the possible influences of uncertainties such as measurement noise and parameter variation on damage location identification. Similar issue has been discussed in Ref. [21], which shows that the index constructed from curvature modes is effective for damage location identification for systems with small parameter variations. Since the two indices proposed in this paper are in the same nature as the one used in [21], one would expect a similar conclusion. In addition, care should be taken during experiment, to enhance the quality of the signals by using standard techniques such as anti-aliasing, filter and "ensemble averaging". Moreover, techniques such as wavelet-based de-noising can also be used to refine rough data before they are used for identification [22].

4. Simulation analyses

A *Matlab* program was developed to demonstrate the strain modal analysis and the damage location identification of a simply supported plate with dimension $a \times b \times h = 1 \times 1.5 \times 0.006$ (non-dimensional) (Fig. 1(b)).

4.1. Strain modal analysis

Assume that the center of the defective area locates at $(0.25a, 0.25b)$ with $a_c/a = 0.1$, $b_c/b = 0.1$ and $h_c/h = 0.2$ (Fig. 1(b), case 1). Let the threshold be $\delta = 5 \times 10^{-3}$ and choose the trail functions as $\varphi_i(x) = \sin(i\pi x/a)$ and $\eta_j(y) = \sin(j\pi y/b)$. According to the analysis described in Section 2 and after computer iterations, the tolerances of $\varepsilon_{r,x}(x,y)$ $(r = 1,\ldots,5)$ will converge to δ if the orders of series are selected as $m = n = 18$. The strain mode shape of the damaged plate can be obtained thereby. Fig. 2(a)–(d) shows plots of the normalized strain mode shapes for modes (1,1) and (1,2) of the intact and damaged cases, respectively. It can be found that when damage occurs at the structure, there is a significant variation at the defective area; and outside this area, change in the strain mode shape is trivial. Obviously, the strain mode shape is a parameter sensitive to local damage.

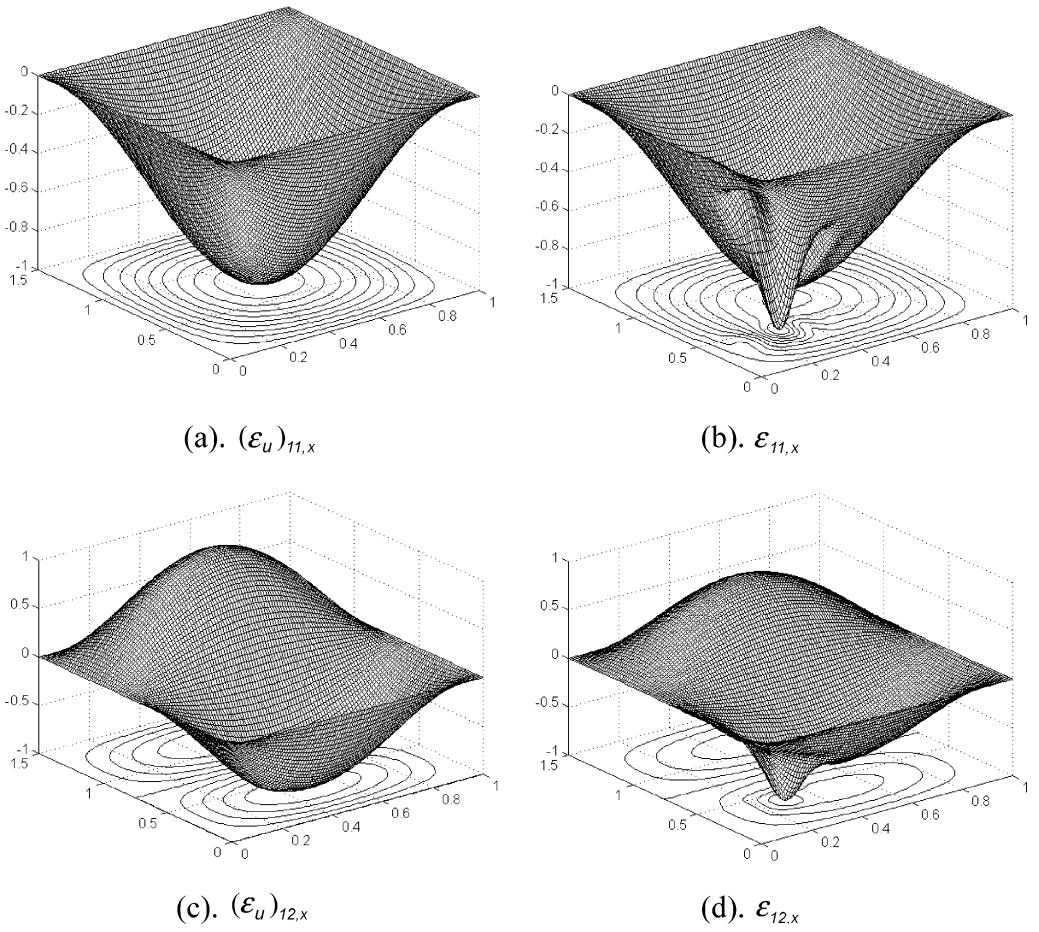

Fig. 2. The normalized strain mode shapes of the intact and damaged cases.

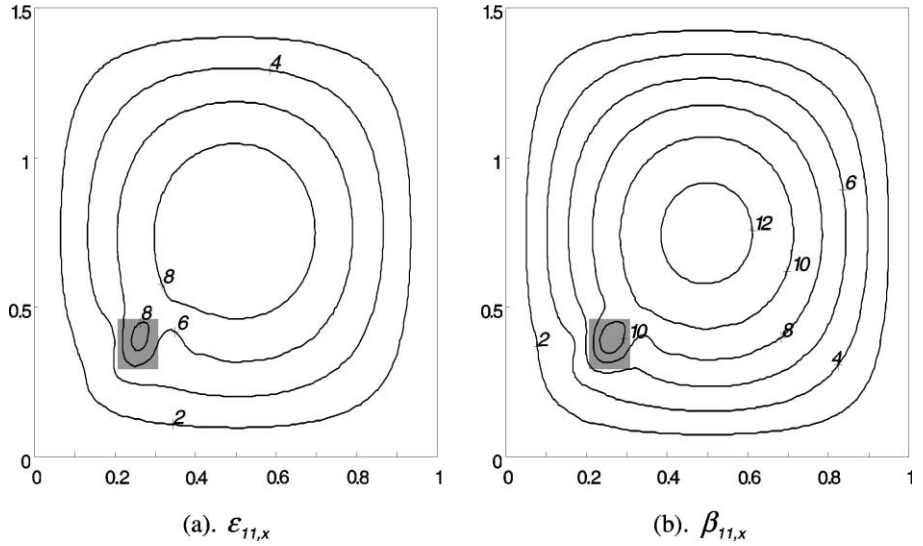

Fig. 3. Contours of constant level for parameters $\varepsilon_{11,x}(x,y)$ and $\beta_{11,x}(x,y)$ with the $\boldsymbol{S}_{\mathrm{d}}$ shown in Fig. 1(b), case 1.

4.2. Sensitivity analysis of damage indices

4.2.1. Sensitivity of parameters $\varepsilon_{r,x}(x,y)$ and $\beta_{r,x}(x,y)$

The contours of constant level of parameters $\varepsilon_{r,x}(x,y)$ and $\beta_{r,x}(x,y)$ for mode (1,1) of the structure with damage shown in case 1 of Fig. 1(b) are plotted in Fig. 3. It can be seen that the maximal values of $\varepsilon_{11,x}(x,y)$ and $\beta_{11,x}(x,y)$ at the defective area (marked with the shadow in figures) are 8 and 10, respectively. This observation is consistent with previous description on the sensitivity analysis of $\beta_{r,x}(x,y)$ and $\varepsilon_{r,x}(x,y)$, i.e., the index defined from the bending moment can give stronger indication of damage locations than that from the strain mode shape.

4.2.2. Sensitivity of damage location indices $\bar{\beta}_{r,x}(x,y)$ and $\Delta\bar{\varepsilon}_{r,x}(x,y)$

In order to investigate the identification capability of the two proposed indices, the contour (or mesh) plots of the bending moment index $\bar{\beta}_{r,x}(x,y)$ and the residual strain mode shape index $\Delta\bar{\varepsilon}_{r,x}(x,y)$ for damage occurring at different locations in the structure are illustrated.

4.2.2.1. Case 1: damage locates away from the nodal line of the structure. Fig. 4(a)–(d) shows the contours of the bending moment index $\bar{\beta}_{r,x}(x,y)$ and the residual strain mode shape index $\Delta\bar{\varepsilon}_{r,x}(x,y)$ for modes (1,1) and (1,2) with the defective area shown in case 1 of Fig. 1(b),

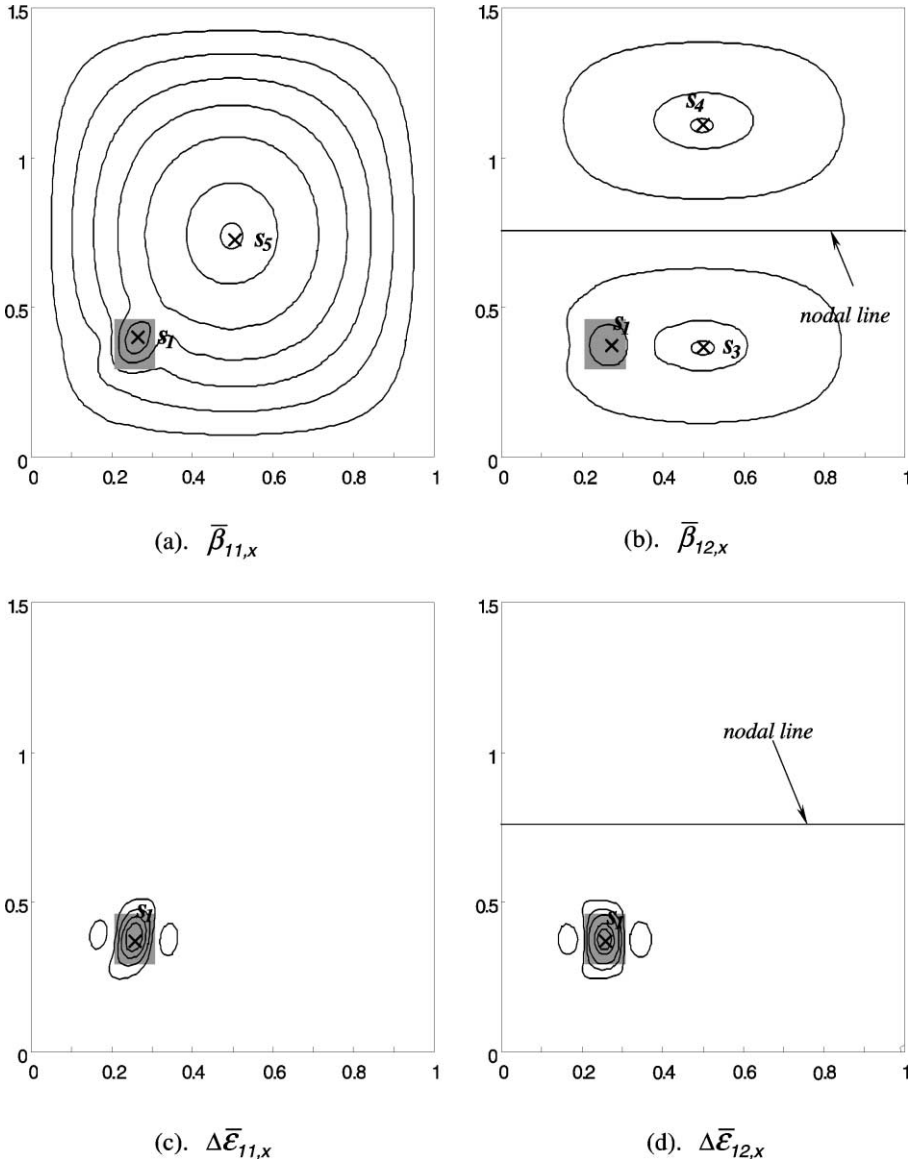

Fig. 4. The bending moment index $\bar{\beta}_{r,x}$ and the residual strain mode shape index $\Delta\bar{\varepsilon}_{r,x}$ with the $\boldsymbol{S}_{\mathrm{d}}$ shown in Fig. 1(b), case 1.

respectively. From Fig. 4(a) and (b), it can be found that the aggregations of $\boldsymbol{S}$ and $(\boldsymbol{S}_{\mathrm{p}})_r$ for $\bar{\beta}_{11,x}(x,y)$ and $\bar{\beta}_{12,x}(x,y)$ are $\boldsymbol{S}=\boldsymbol{S}_{11}\cup\boldsymbol{S}_{12}=\{s_1,s_3,s_4,s_5\}$, $(\boldsymbol{S}_{\mathrm{p}})_{11}=\{s_5\}$ and $(\boldsymbol{S}_{\mathrm{p}})_{12}=\{s_3,s_4\}$. According to the identification using the bending moment index, when s_i locates at the position s_1, the condition $s_i\cap(\boldsymbol{S}_{\mathrm{p}})_{11}\cap(\boldsymbol{S}_{\mathrm{p}})_{12}=\emptyset$ is satisfied. This means that s_1 is the location of damage, while s_5 and (s_3,s_4) are the locations of peaks for modes (1,1) and (1,2) only. In Fig. 4(c) and (d), the influence of peaks caused by modes is vanished, and the maximum of the residual strain mode shape appears at the defective area. It also can be seen that the number and location of peaks are independent of the mode selected for analysis, i.e., no matter which mode is selected for analysis, the damage location can always be identified accurately.

4.2.2.2. Case 2: damage locates at the nodal line of the structure. In Fig. 5(a)–(d), the contours of $\bar{\beta}_{r,x}(x,y)$ and $\Delta\bar{\varepsilon}_{r,x}(x,y)$ for modes (1,1) and (1,2) with the defective area shown in case 2 of Fig. 1(b) are plotted, respectively. For the bending moment index, damage site locating at s_2 is accurately identified from $\bar{\beta}_{11,x}(x,y)$. From $\bar{\beta}_{12,x}(x,y)$, however, no peak is observed at s_2, because s_2 locates at the nodal line of that mode. This gives guidance on damage detection during experimental tests, i.e., more than one modes need to be measured to avoid 'neglected alarm' using the bending moment index. As to

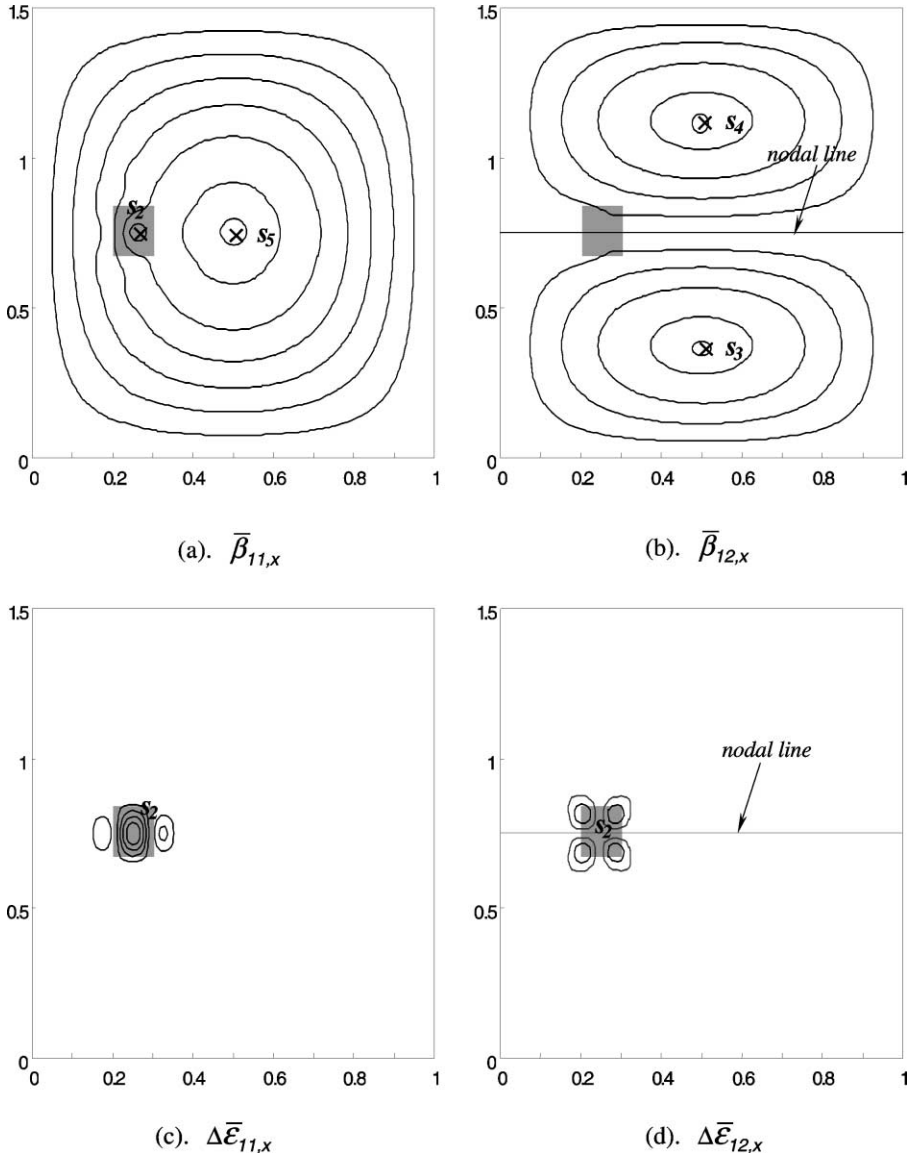

Fig. 5. The bending moment index $\bar{\beta}_{r,x}$ and the residual strain mode shape index $\Delta\bar{\varepsilon}_{r,x}$ with the $\boldsymbol{S}_{\mathrm{d}}$ shown in Fig. 1(b), case 2.

the residual strain mode shape index, change in mode shapes at s_2 is observed remarkably. Although the number and locations of peaks are variable for different modes, for example, *three* peaks for mode (1,1) and *four* peaks for mode (1,2), they appear around s_2 (Fig. 5(c) and (d)). Thus, it is summarized that the proposed indices are valid even if damage occurs at the nodal line of the structure.

4.2.2.3. Case 3: damage locates at the center of the structure. A special case to be discussed is for damage locating at the center of the structure (s_5). As is known, for a given mode (i,j), s_5 will be the location of peak of that mode when both (i,j) are odd; otherwise, s_5 will be the location of nodal line. In such case, the identification capability of $\bar{\beta}_{r,x}(x,y)$ and $\Delta\bar{\varepsilon}_{r,x}(x,y)$ on damage location is of interest. In results presented hereafter, instead of the damage indices (Eqs. (17) and (22)), the sensitive parameters (Eqs. (9) and (20)) are used for the sake of convenience. Fig. 6(a)–(d) shows the mesh plots of the normalized $\beta_{r,x}(x,y)$ and $\Delta\varepsilon_{r,x}(x,y)$ for modes (1,2) and (2,2) with the defective area shown in case 3 of Fig. 1(b), respectively. No obvious peak is found at the defective area from $\beta_{r,x}(x,y)$, while the variation is significant and peaks are observed from $\Delta\varepsilon_{r,x}(x,y)$. Consequently, the residual strain mode shape index is more sensitive to location identification than the bending moment index for damage locating at the center of the structure.

4.2.2.4. Case 4: multiple damage in the structure. Theoretically speaking, when more than one damage occurring in the structure, the bending moment index and the residual strain mode shape index should be effective for damage detection because of the local characteristic of strain mode. Fig. 7(a)–(d) plots the mesh of the normalized $\beta_{r,x}(x,y)$ and $\Delta\varepsilon_{r,x}(x,y)$ for modes (1,2) and (2,2) when the structure is subjected to two damage (Fig. 1(b), case 4). Evidently, damage occurring at s_1 and s_6 are accurately detected. This demonstrates the flexibility of the adopted indices for multi-damage location identification.

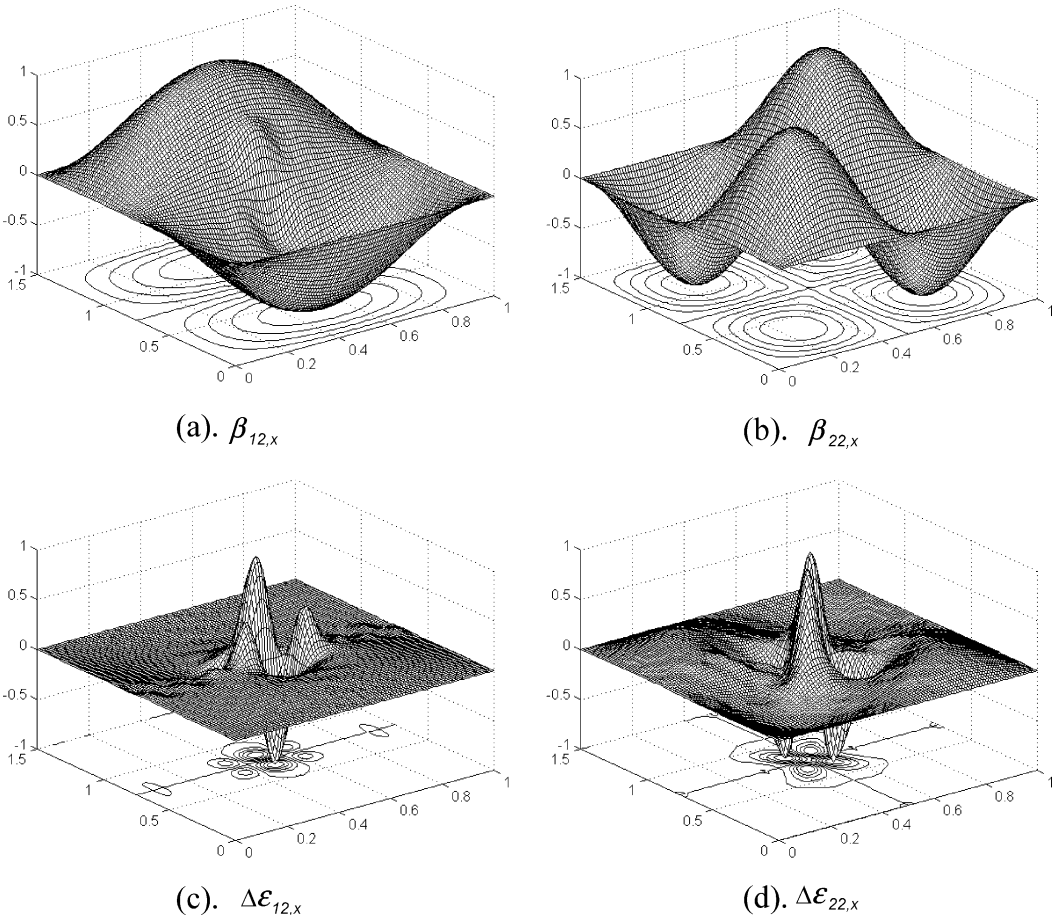

Fig. 6. The normalized bending moment $\beta_{r,x}$ and the residual strain mode shape $\Delta\varepsilon_{r,x}$ with the $\boldsymbol{S}_{\mathrm{d}}$ shown in Fig. 1(b), case 3.

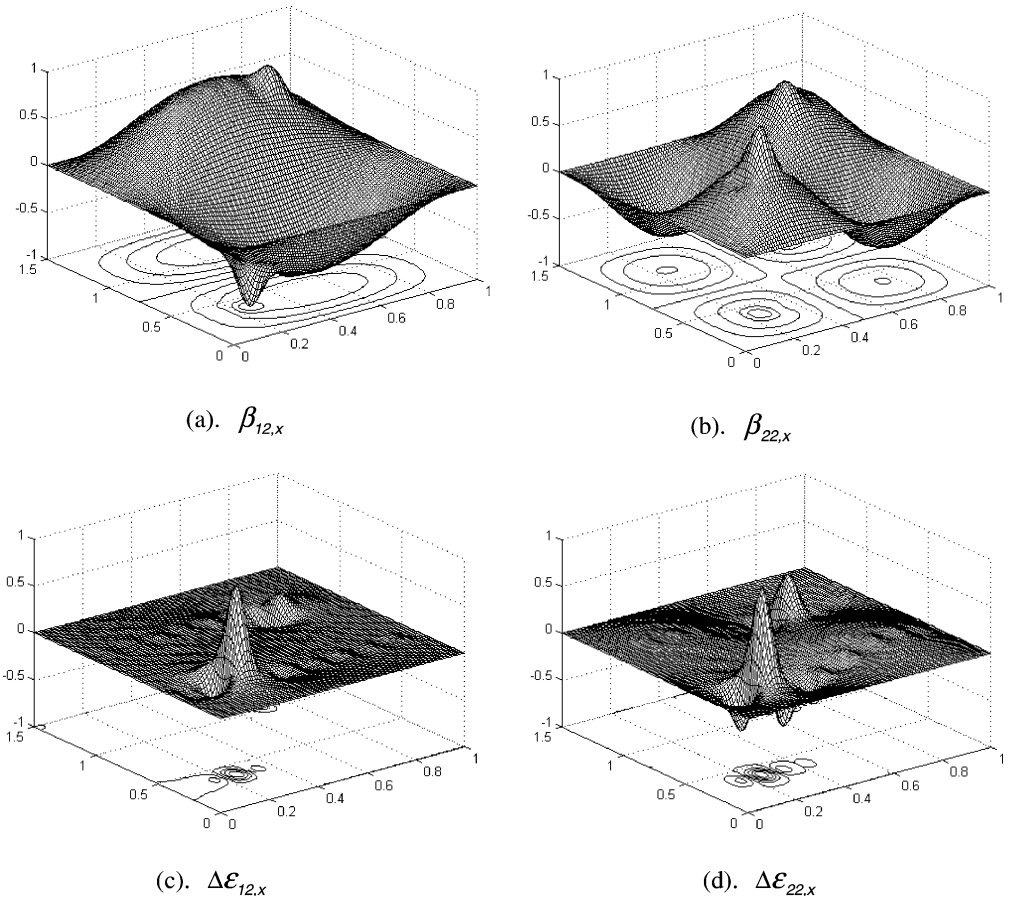

Fig. 7. The normalized bending moment $\beta_{r,x}$ and the residual strain mode shape $\Delta\varepsilon_{r,x}$ for the structure with two damage shown in Fig. 1(b), case 4.

5. Experimental verifications

Experimental tests using aluminum plates with free boundary conditions were conducted. To create the free boundary condition, the plates were suspended from a stiff steel frame by two nylon bands of very weak stiffness. The dimension of the damaged plate is the same as that of the intact plate with $a \times b \times h = 330 \times 240 \times 2$ mm^3, and the defective area locates at the region Ω: $35 \leqslant x \leqslant 65$ mm, $60 \leqslant y \leqslant 90$ mm with $h_c/h = 0.5$.

Fig. 8(a) shows the experimental set-up used for testing. A sinusoidal signal was generated by a signal generator (TGA 1230), then amplified by a Piezo-Driver (Trek Model 700), and exerted on the test structures through a pair of piezoceramic actuators (Sensortech MB400) [23]. The strain amplitudes in both x and y directions were sensed by strain gauges (FLA-6-11, using the half bridge connection) and processed by the strain data logger (MGCplus). The *first* (mode (1,1)) and *third* (mode (2,1)) natural frequencies of the intact and damaged plates were first measured using the frequency response functions, i.e., $\omega_{11} = 81.5$ Hz and $\omega_{21} = 182$ Hz for the intact plate, and $\omega_{11} = 81$ Hz for mode (1,1) and $\omega_{21} = 181.5$ Hz for the damaged plate. Then, the frequencies of excitation signals were set as the corresponding resonant frequencies of each analyzed modes to ensure that the most strain information of the analyzed modes can be obtained. The amplitudes of $\varepsilon_{r,x}(x,y)$ and $\varepsilon_{r,y}(x,y)$ at 12 locations (Fig. 8(b)) were measured to construct indices $\bar{\beta}_{r,x}(x,y)$ and $\Delta\bar{\varepsilon}_{r,x}(x,y)$ for modes (1,1) and (2,1).

The variation of $\bar{\beta}_{r,x}(x,y)$ at all 12 measuring points has been experimentally tested. Using a cross section $\boldsymbol{A}$–$\boldsymbol{A}$, passing through the defective area as an example, both experimental and simulation results at $(s_1, s_2, s_4, s_8, s_{12})$ for modes (1,1) and (2,1) are shown in Fig. 9(a) and (b) for comparison. Numerical simulation for the intact plate is also given for reference. The experimental data are all normalized with respect to the maximum value. It can be seen that good agreement between simulation and experiment is achieved, i.e., $\bar{\beta}_{r,x}(x,y)$ decreases at the defective area, and outside this area, no

(a). Experimental setup

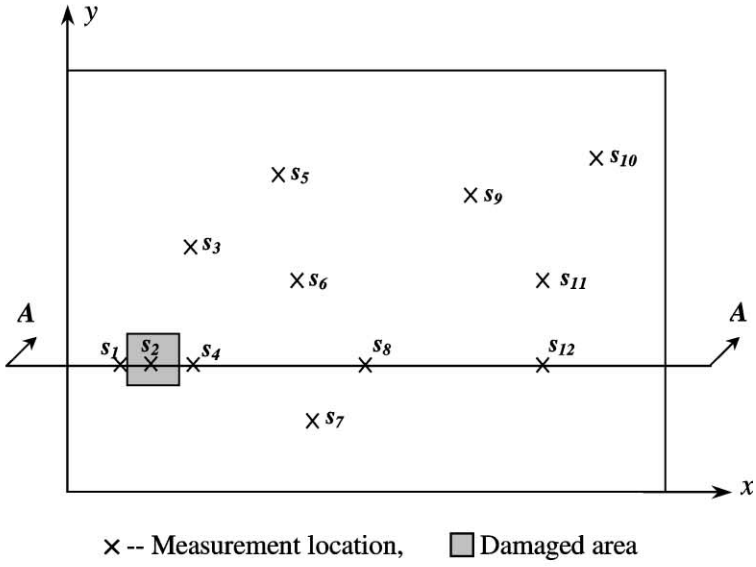

(b). The tested plate

Fig. 8. Experimental set-up.

obvious change is observed. It clearly shows that $\bar{\beta}_{r,x}(x,y)$ is an effective index for damage location identification.

Fig. 9(c) and (d) shows the histogram of residual strain mode shape index $\Delta\bar{\varepsilon}_{r,x}(x,y)$ at locations (s_1–s_{12}) for modes (1,1) and (2,1), respectively. It can be found that *three* significant peaks of $\Delta\bar{\varepsilon}_{r,x}(x,y)$ can be observed. The largest one appears at s_2, i.e., at the defective area, and the other two appear at s_1 and s_4, i.e., both locating near the defective area. Apart from these locations, the values of $\Delta\bar{\varepsilon}_{r,x}(x,y)$ are relatively small. Apparently, the index $\Delta\bar{\varepsilon}_{r,x}(x,y)$ is sensitive to damage. Experimental results are therefore consistent with numerical simulations.

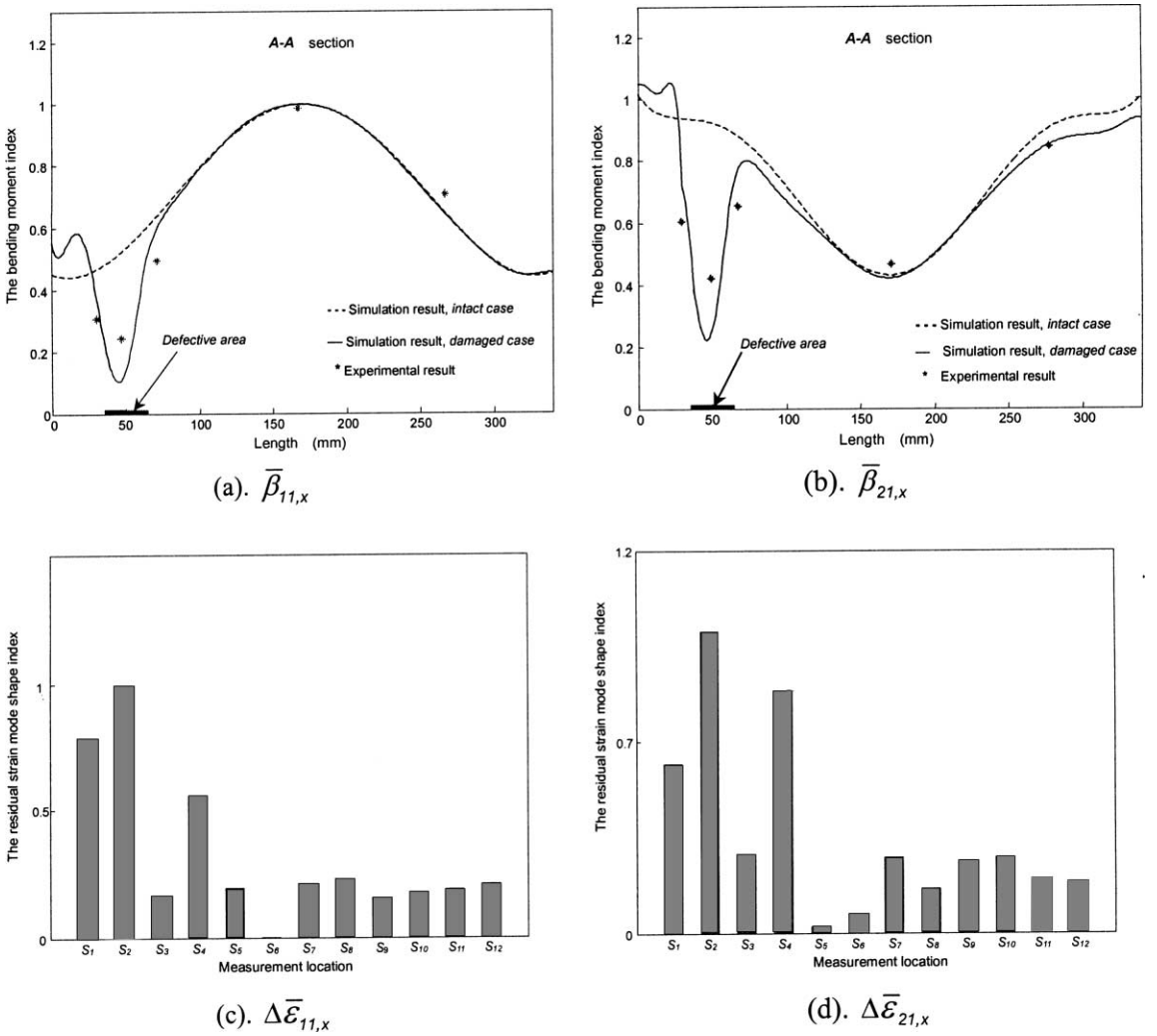

Fig. 9. The bending moment index $\bar{\beta}_{r,x}$ and the residual strain mode shape index $\Delta\bar{\varepsilon}_{r,x}$.

6. Conclusions

Identification of damage location of plate-like structures using strain mode technique has been investigated, and two novel sensitive damage indices—the bending moment index and the residual strain mode shape index, have been proposed in this paper. In order to construct these indices from the strain modal parameter, strain modal analysis of the damaged structure is performed, and the strain mode shape is derived based on the Rayleigh–Ritz approach. Comparing with the conventional indices, the proposed indices are intuitive and easy to be realized in practical applications.

For the bending moment index, no baseline information is required during the identification process. Obviously, this is a simple way because only the strains of the damaged case need to be measured during vibration tests. Sensitivity analysis of the parameters of the strain mode shape and the bending moment reveals that the parameter of bending moment is more sensitive than that of strain mode shape, and can give strong indication on damage locations. In using this index, more than *one* mode should be used for identification, and care should be taken to avoid the problem of neglect alarm, which may happen, for example, when damage occurs at the center of the structure.

For the residual strain mode shape index, due to the use of mode subtraction technique, the effects of peaks and nodal lines caused by modes can be eliminated. Damage sites in the structure can therefore be identified accurately no matter where damage will occur. It is an effective way to locate damage sites by measuring the strain information of the intact and damaged structures using the strain gauges attached at the critical areas of

the structure. However, the use of this index requires the information of strains of the intact structure. Numerical simulation and experimental analysis show that both proposed indices can provide fairly good indication results of structural damage locations identification.

Acknowledgements

This research is sponsored by the Research Committee of the Hong Kong Polytechnic University (Grant: GYY-27) and the Scientific Research Foundation for the Returned Overseas Chinese Scholars, State Education Ministry.

References

[1] Doebling SW, Farrar CR, Prime MB, Shevitz SW. Damage identification and health monitoring of structural and mechanical systems from changes in their vibration characteristics: a literature review. Los Alamos National Laboratory Report LA-13070-VA5, 1996.
[2] Chang FK. Structural health monitoring: current status and perspectives. Lancaster, Pennsylvania: Technomic publishing; 1997.
[3] Zou Y, Tong L, Steven GP. Vibration-based model-dependent damage (delamination) identification and health monitoring for composite structures—a review. J Sound Vib 2000;230:357–78.
[4] Stubbs N, Kim JT. Damage localization in structures without baseline modal parameters. AIAA J 1996;34:1644–9.
[5] Chen HP, Bicanic N. Assessment of damage in continuum structures based on incomplete modal information. Comput Struct 2000;74:559–70.
[6] Shi ZY, Law SS, Zhang LM. Structural damage localization from modal strain energy change. J Sound Vib 1998;218:825–44.
[7] Friswell MI, Penny JET, Garvey SD. A combined genetic and eigensensitivity algorithm for the location of damage in structures. Comput Struct 1998;69:547–56.
[8] Ahmadian H, Mottershead JE, Friswell MI. Damage location indicators from substructure mode shapes. Inverse Probl Eng 2000;8:309–23.
[9] Cornwell P, Doebling SW, Farrar CR. Application of the strain energy damage detection method to plate-like structures. J Sound Vib 1999;224:359–74.
[10] Dems K, Mroz Z. Identification of damage in beam and plate structures using parameter-dependent frequency changes. Eng Comput 2001;18:96–120.
[11] Wang ML, Heo G, Satpathi D. A health monitoring system for large structural systems. Smart Mater Struct 1998;7:606–16.
[12] Yam LH, Li DB, Leung TP, Xue KZ. Experimental study on modal strain analysis of rectangular thin plates with small holes. In: Proceedings of the 12th International Modal Analysis Conference, Honolulu, Hawaii. 1994. p. 1415–8.
[13] Yam LH, Leung TP, Li DB, Xue KZ. Theoretical and experimental study of modal strain analysis. J Sound Vib 1996;192:251–60.
[14] Pandey AK, Biswas M, Samman MM. Damage detection from changes in curvature mode shapes. J Sound Vib 1991;145:321–32.
[15] Yao GC, Chang KC, Lee GC. Damage diagnosis of steel frames using vibrational signature analysis. J Eng Mech—ASCE 1992;118(9):1949–61.
[16] Abdel Wahab MM, De Roeck G. Damage detection in bridges using modal curvatures: Application to a real damage scenario. J Sound Vib 1999;226:217–35.
[17] Ratcliffe CP, Bagaria WJ. Vibration technique for locating delamination in a composite beam. AIAA J 1998;36:1074–7.
[18] Swamidas ASJ, Chen Y. Monitoring crack-growth through change of modal parameters. J Sound Vib 1995;186:325–43.
[19] Reddy JN. Mechanics of laminated composite plates: theory and analysis. Boca Raton, Florida: CRC Press; 1997.
[20] Bazant ZP, Cedolin L. Stability of structures: elastic, inelastic, fracture, and damage theories. New York: Oxford University Press; 1991.
[21] Li YY, Yam LH. Sensitivity analyses of sensor locations for vibration control and damage detection of thin-plate systems. J Sound Vib 2001;240:623–36.
[22] Kim YY, Hong JC, Lee NY. Frequency response function estimation via a robust wavelet de-noising method. J Sound Vib 2001;244:635–49.
[23] Proulx B, Cheng L. Dynamic analysis of piezoceramic actuation effects on plate vibrations. Thin-walled Struct 2000;37:147–62.